ISSN 1027-4510, Journal of Surface Investigation: X-ray, Synchrotron and Neutron Techniques, 2017, Vol. 11, No. 3, pp. 549–553. © Pleiades Publishing, Ltd., 2017.
Original Russian Text © S.N. Nikolaev, K.Yu. Chernoglazov, V.A. Demin, N.K. Chumakov, V.A. Levanov, A.A. Magomedova, A.V. Sitnikov, Yu.E. Kalinin, A.B. Granovskii, V.V. Rilkov, 2017, published in Poverkhnost', 2017, No. 5, pp. 76–81.

Conductivity and Anomalous Hall Effect in Film Magnetic Nanocomposites Based on Nonstoichiometric Oxides

S. N. Nikolaev[a, *], K. Yu. Chernoglazov[a, **], V. A. Demin[a], N. K. Chumakov[a], V. A. Levanov[a, b], A. A. Magomedova[b], A. V. Sitnikov[c], Yu. E. Kalinin[c], A. B. Granovskii[b, d], and V. V. Rilkov[a, d]

[a] *National Research Center "Kurchatov Institute," Moscow, 123182 Russia*
[b] *Moscow State University, Moscow, 119991 Russia*
[c] *Voronezh State Technical University, Voronezh, 394026 Russia*
[d] *Institute of Theoretical and Applied Electrodynamics, Russian Academy of Sciences, Moscow, 127412 Russia*
**e-mail: niklser@list.ru*
***e-mail: expe28@gmail.com*

Received August 22, 2016

Abstract—The transport properties of film nanocomposites $(Co_{40}Fe_{40}B_{20})_x(AlO_y)_{100-x}$ and $(Co_{84}Nb_{14}Ta_2)_x(AlO_y)_{100-x}$ based on AlO_y oxide ($y \sim 1$), containing a ferromagnetic metal, are studied in the region of the metal–insulator transition ($57 > x > 47$ at %). It is found that at $x > 49$ at %, the conductivity of nanocomposites is well described by a logarithmic law of $\sigma(T) = a + b\ln T$, which can be explained by the peculiarities of the Coulomb interaction in nanogranular systems with metallic conductivity near the metal–insulator transition. It is shown that parameter b is determined by the characteristic size of the percolation cluster cell, which in nanocomposites of both types happen to be the same (~8 nm) and correlates well with the results of electron microscopy studies. The temperature dependence of the anomalous Hall effect at the logarithmic dependence of conductivity is studied for the first time. In the immediate vicinity of the transition, a power-law scaling between the anomalous Hall resistance and longitudinal resistance $\rho_H^a \propto \rho^{0.4}$, is detected, which can be explained by the suppression of its own mechanism of the anomalous Hall effect under the strong scattering of charge carriers.

Keywords: magnetic nanogranular composites, metal–insulator transition, conductivity, anomalous Hall effect

DOI: 10.1134/S1027451017030132

INTRODUCTION

Magnetic metal–insulator composites are an ensemble of ferromagnetic nanogranules tightly packed into a dielectric matrix, the electronic and magnetic properties of which can be controlled at the nanoscale level [1–3]. Increased interest in such systems arose after the discovery of a giant magnetoresistance effect in them, which is most pronounced on the dielectric side of the percolation transition [4] and can be used to create magnetic sensors. It was also found that these materials might have an increased coercive force, which is needed to create superdense magnetic memory, high values of the magneto-optical characteristics, good absorption capacity of electromagnetic radiation, and other properties interesting for practical applications [1–3].

In the case of magnetic nanocomposites based on nonstoichiometric oxides, the effect of resistive switching (along with magnetoresistive switching) can be observed under the effect of an electric field, which is caused, presumably, by the movement of oxygen vacancies in the insulator and can be used to create multipurpose memristor devices [5].

Scientific interest in granular magnetic nanocomposites can also be explained by the fact that they are an unusual example of percolation systems with properties determined by interrelated disorder effects, Coulomb and magnetic interactions, electron correlations, and size quantization [1–3]. In such systems, an unusual logarithmic temperature dependence of the conductivity $\sigma(T)$ can be observed near the metal–insulator transition, not associated with the effects of weak localization, which was explained recently by some features of the Coulomb interaction in nanogranular alloys [2, 6]:

$$\sigma(T) = a + b\ln T, \quad (1)$$

where a and b are certain constants depending, in particular, on the structural parameters of the nanocomposite.

In the present paper, the transport properties of film nanocomposites $(Co_{40}Fe_{40}B_{20})_x(AlO_y)_{100-x}$ and $(Co_{84}Nb_{14}Ta_2)_x(AlO_y)_{100-x}$ based on nonstoichiometric AlO_y oxide ($y \sim 1$), containing a ferromagnetic metal, are studied in the region of the metal–insulator transition ($56 > x > 30$ at %). It is found that at a metal concentration of $x > 49$ at %, the conductivity of nanocomposites is well described by a logarithmic law (Eq. (1)). The slope of the dependences of b, determined by the characteristic size of "the lattice constant" of conductive cluster D [2], happened to be the same in nanocomposites of both types; it is slightly dependent on x. Using [2], the value of D was estimated to be ~8 nm. It is important that the value of D is obtained near the metal–insulator transition, where the conductivity is determined by the fractal structure of the granular nanocomposite, and therefore, the size of a percolation cluster cell is difficult to estimate by electron microscopy.

The results of studying the temperature behavior of the anomalous Hall effect in order to identify its mechanism are also presented.

EXPERIMENTAL

Film nanocomposites $(Co_{40}Fe_{40}B_{20})_x(AlO_y)_{100-x}$ and $(Co_{84}Nb_{14}Ta_2)_x(AlO_y)_{100-x}$ with a thickness of $l \approx 2.7$ and 1 μm, respectively, were obtained by the ion beam sputtering of composite targets, namely, substrates of ferromagnetic alloys, on the surface of which 12 alumina plates were placed with gradually varying distance between them [7]. Such a composite target yielded composites with a controlled variation in the concentration of the metal and dielectric components in the range of $x = 25–60$ at % in one technological cycle. The elemental composition of the films was determined using a JEOL JSM-6380 LV scanning electron microscope equipped with an Oxford INCA Energy 250 energy dispersive X-ray device. The composite was deposited on pyroceramic substrates 60 × 48 mm in size; the temperature during deposition did not exceed 393 K.

To study the conductivity and the Hall effect, we prepared samples in the shape of a double Hall cross using photolithography, with a conducting channel width of $W = 1.2$ mm and a distance between potential probes on the lateral faces of the sample of $L = 1.4$ mm.

The transport properties (conductivity and the Hall effect) were examined using an automated installation via an evacuated insert with a superconducting solenoid, immersed in a helium Dewar vessel, in the temperature range of 10–300 K in a magnetic field of 2 T.

Due to the percolation nature of conductivity, magnetic nanocomposites are a strongly heterogeneous system. For this reason, there is always a noticeable voltage between the Hall probes in the samples under study, even in the absence of magnetic field B, which is associated with asymmetry of the percolation net and independent on the sign of B. Therefore, the Hall resistance R_H was determined by the difference between the measured values of the transverse resistance $R_{xy} = V_y/I_x$, corresponding to the positive and negative direction of the magnetic field: $R_H = [R_{xy}(+B) - R_{xy}(-B)]/2$, where V_y was the voltage between the Hall probes, and I_x is the current flowing through the sample.

RESULTS AND DISCUSSION

Temperature dependence of the conductivity. Figure 1a demonstrates the temperature dependences of the conductivity $\sigma(T)$ of the film nanocomposite $(Co_{40}Fe_{40}B_{20})_x(AlO_y)_{100-x}$ (curves *1–4*) and $(Co_{84}Nb_{14}Ta_2)_x(AlO_y)_{100-x}$ (curves *5–7*) with different concentrations of ferromagnetic alloy ($x = 47–57$ at %) in coordinates $\sigma–\ln T$. It is seen that in the range of $x = 49–57$ at %, the temperature dependence of $\sigma(T)$ is well described by a logarithmic law. However, at $x < 49$ at %, a metal–insulator transition takes place. At $x = 47$ at %, the dependence of $\sigma(T)$ is of the activation type: $\ln\sigma \propto (T_0/T)^{1/2}$ (Fig. 1b). This dependence is often observed in granular nanocomposites in the dielectric region of compositions [2]. Of note is the proximity of the slopes of the logarithmic dependences conductivity σ for samples of both types. For $(Co_{40}Fe_{40}B_{20})_x(AlO_y)_{100-x}$ and $(Co_{84}Nb_{14}Ta_2)_x(AlO_y)_{100-x}$, with x decreasing from 56–57 to 53 at %, the slope of $d\sigma/d\ln T$ varies from 32 to 26 $(\Omega\ \text{cm})^{-1}$ and from 33 to 29 $(\Omega\ \text{cm})^{-1}$, respectively.

Let us assess the slope of the dependences of σ from ln T by means of the model [2, 6]. Below the percolation threshold, when tunneling conduction between granules G_t exceeds the conduction quantum $g = G_t/(2e^2/\hbar) > 1$, the conductivity of the metal–insulator nanocomposite, according to [2], obeys the equation

$$\sigma(T) = \sigma_0\left(1 - \frac{1}{2\pi dg}\ln\left[\frac{gE_C}{k_BT}\right]\right) = \sigma_0\left(1 - \frac{1}{\pi zg}\ln\left[\frac{gE_C}{k_BT}\right]\right) = \sigma_0\left(1 - \alpha_C\ln\left[\frac{gE_C}{k_BT}\right]\right). \quad (1)$$

Here, d is the dimension of the system; z is the coordination number ($z = 6$ for a cubic lattice); E_C is the Coulomb energy upon the addition of one electron to the granule. Assuming that tunneling conduction is related to the effective (measured) conductivity by the ratio of $G_t \approx \sigma_0\frac{D^2}{D} = \sigma_0 D$, we obtain the relationship between σ_0 and the normalized conductance g [2], that is,

$$\sigma_0 = \frac{2e^2g}{\hbar D}, \quad (2)$$

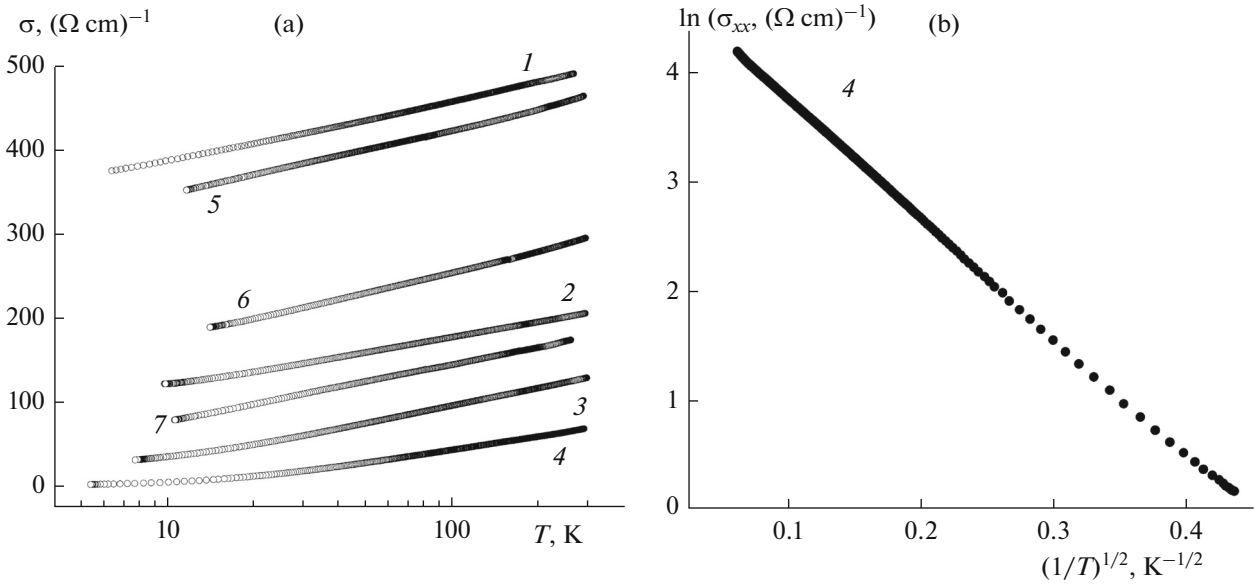

Fig. 1. (a) Temperature dependence of the conductivity $\sigma(T)$ of nanocomposites (*1*–*4*) $(Co_{40}Fe_{40}B_{20})_x(AlO_y)_{100-x}$ and (*5*–*7*) $(Co_{84}Nb_{14}Ta_2)_x(AlO_y)_{100-x}$ with different concentrations of a ferromagnetic alloy: (*1*) 56, (*2*) 53, (*3*) 49, (*4*) 47, (*5*) 57, (*6*) 55.2, and (*7*) 52.8 at %; (b) dependence of ln σ on $(1/T)^{1/2}$ of $(Co_{40}Fe_{40}B_{20})_x(AlO_y)_{100-x}$, $x = 47$ at %.

where D is the characteristic size ("lattice constant") of a percolation cluster cell. In the simplest case, $D \approx a$, that is, the size of a granule [2], when the thickness of the tunneling layers $s \ll a$.

By substituting Eq. (3) into Eq. (2), we find the slope of the logarithmic dependence of the conductivity

$$\sigma_0\alpha_c[(\Omega\,\mathrm{cm})^{-1}] = \frac{2e^2}{\hbar\pi z D} = 1.55\times10^{-4}(zD\ [\mathrm{cm}])^{-1}. \quad (3)$$

That is, the slope is determined by the characteristic size of a percolation cluster cell, which, strictly speaking, cannot be measured by electron microscopy near the percolation threshold.

It has been recently shown [8] that the conditions of applicability of the model [2, 6] (that is, $g > 1$) are met better at high metal concentrations of ~56 at %. Substituting the magnitudes of the slope of the logarithmic dependences, found above, into Eq. (4), we obtain for $z = 6$ typical cell sizes of $D \approx 8.1$ and 7.8 nm for nanocomposites $(Co_{40}Fe_{40}B_{20})_x(AlO_y)_{100-x}$ and $(Co_{84}Nb_{14}Ta_2)_x(AlO_y)_{100-x}$, respectively. We note that the obtained values of D correlate well with the grain size typical of this type of nanocomposites, which, according to electron microscopy studies, varies from 2–3 to 5–7 nm with the metal concentration increasing from 30–34 to 50–59 at % [3]. It can be concluded that the conducting chains, forming a cluster, are composed of one or two tunnel junctions formed by nanogranules of ferromagnetic alloys.

Anomalous Hall effect. Studies concerning the anomalous Hall effect are prominent in investigations of ferromagnetic systems, especially disordered ones [9]. This effect is determined by the spin–orbital interaction and the spin polarization of charge carriers, when the Hall resistance of a magnet is described by the sum of two terms:

$$R_\mathrm{H} = \frac{R_0}{l}B + \frac{R_\mathrm{s}}{l}M = R_\mathrm{H}^\mathrm{n} + R_\mathrm{H}^\mathrm{a}, \quad (4)$$

where l is the thickness of the layer of magnetic material; R_0 is the constant of the normal Hall effect caused by the Lorentz force; B is the magnetic induction; R_s is the constant of the anomalous Hall effect, determined by the effect of spin-orbital interaction on the transport of spin-polarized charge carriers; M is the magnetization; $R_\mathrm{H}^\mathrm{n} = \rho_\mathrm{H}^\mathrm{n}/l$ and $R_H^\mathrm{a} = \rho_H^\mathrm{a}/l$ are the resistance components of the normal and anomalous Hall effects, respectively.

To identify the mechanism of the anomalous Hall effect, the dependence of the anomalous component of the specific Hall resistance $\rho_\mathrm{H}^\mathrm{a}$ on the longitudinal resistivity $\rho_{xx} = \rho$ is usually studied; that is, the so-called scaling behavior of the anomalous Hall effect $\rho_\mathrm{H}^\mathrm{a} \propto \rho^m$, where m is the exponent determined by the mechanism of the anomalous Hall effect [2]. In metal systems at low temperatures, $m = 1$ in the case of the asymmetric scattering mechanism and $m = 2$ for the lateral shift mechanism and the intrinsic mechanism of the anomalous Hall effect [2]. However, this classification of mechanisms of the effect is not applicable

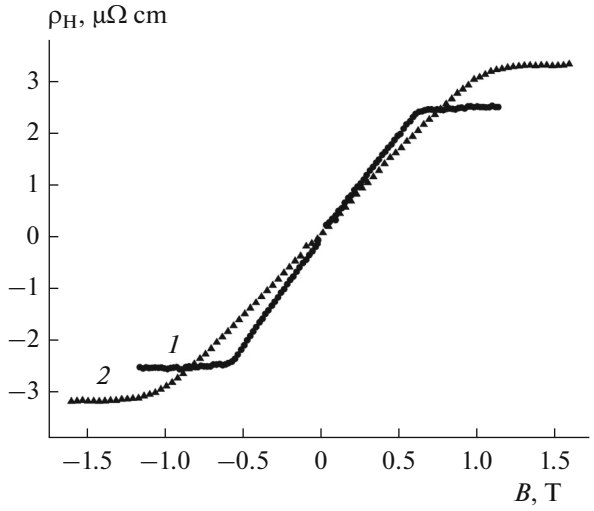

Fig. 2. Dependences of the specific Hall resistance σ_H on the magnetic field of samples (*1*) $(Co_{84}Nb_{14}Ta_2)_x(AlO_y)_{100-x}$, $x = 57$ at %, at 21 K and (*2*) $(Co_{40}Fe_{40}B_{20})_x(AlO_y)_{100-x}$, $x = 56$ at %, at 10 K. For convenience of comparison, the values of ρ_H values at 21 K (curve *1*) are increased twofold.

to highly disordered magnetic materials with low conductivity $\sigma < 10^4\ \Omega^{-1}\ cm^{-1}$, in which scaling of another type was discovered relatively recently [10–13], that is, $\rho_H^a \propto \rho^m$ with $m \approx 0.4$. Scaling is often expressed through the Hall conductivity as $\sigma_H^a = \rho_H^a/\rho^2 = \rho_H^a\sigma^2$. In this representation, $\sigma_H^a \propto \sigma^\gamma$, and $\gamma \approx 1.6$. In the case of "contaminated" metal systems, such scaling is explained by the suppression of the intrinsic mechanism of the anomalous Hall effect under the strong scattering of charge carriers [14]. Such scaling can be expected in the case of the nanocomposites under study, because of their low conductivity $\sigma < 5 \times 10^2\ \Omega^{-1}\ cm^{-1}$ (Fig. 1).

The dependences of the Hall resistance on the magnetic field $\rho_H(B)$ for $(Co_{40}Fe_{40}B_{20})_x(AlO_y)_{100-x}$ ($x = 57$ at %) and $(Co_{84}Nb_{14}Ta_2)_x(AlO_y)_{100-x}$ ($x = 56$ at %) were measured at temperatures of 21 and 10 K, respectively (Fig. 2). It is evident that in fields up to ~0.5 T (curve *1*) and ~1 T (curve *2*) the magnitude of ρ_H varies linearly with the field. In both cases, the films have easy-plane anisotropy. Above 1 T, the magnetization is saturated. The specific resistance ρ_H stops depending on the field, indicating that the anomalous Hall effect makes a dominant contribution to the nanocomposites under study, that is, $R_H^a \gg R_H^n$, and the measured Hall resistance $R_H \approx R_H^a$ (Eq. (4)).

The temperature dependences of the transverse and longitudinal resistance R_{xy} were measured in the temperature range of 10–200 K in different directions of the magnetic field of 1.5 T. The Hall resistance was found from the difference between the values of R_{xy}: $R_H = [R_{xy}(T, +1.5\ T) - R_{xy}(T, -1.5\ T)]/2$. Figure 3 shows the dependences of the anomalous component of the Hall resistance ρ_H^a on the longitudinal resistance $\rho(T)$ in the double logarithmic scale for two samples of $(Co_{40}Fe_{40}B_{20})_x(AlO_y)_{100-x}$: with $x = 56$ at % (Fig. 3a) (immediately after the percolation transition) and $x = 49$ at % (Fig. 3b) (near the metal–insulator transition). In both cases, scaling is observed in the behavior of the anomalous component of the Hall resistance with exponents $m \approx 0.58$ (Fig. 3a) and 0.38 (Fig. 3b). The dependence $\rho_H^a \propto \rho^m$ with $m = 0.6$–0.7

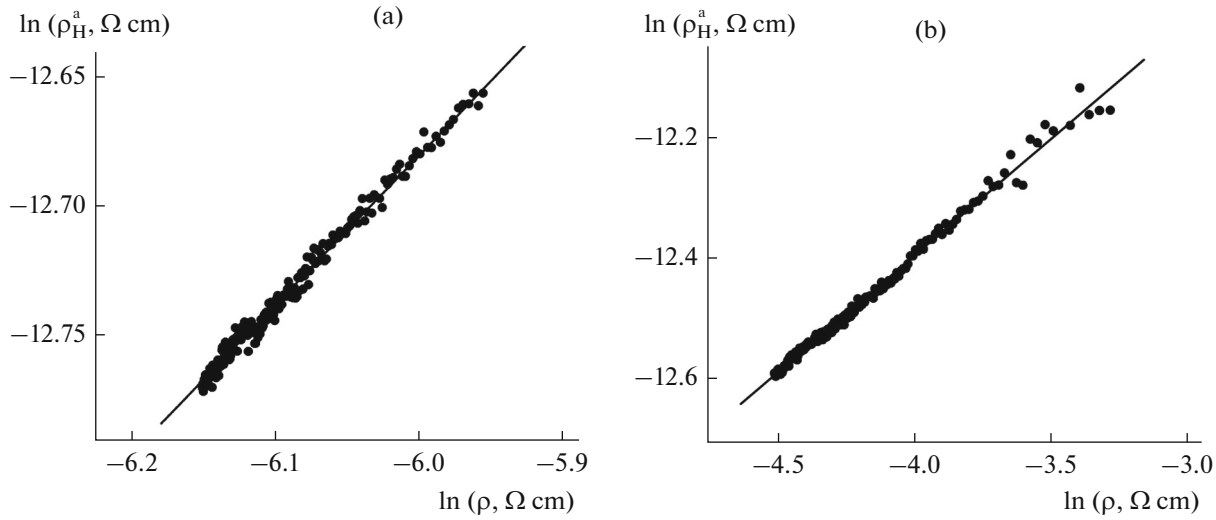

Fig. 3. Dependences of the anomalous component of the Hall resistance ρ_H on the longitudinal resistance ρ of the nanocomposite $(Co_{40}Fe_{40}B_{20})_x(AlO_y)_{100-x}$ with $x =$ (a) 56 at % and (b) 49 at %, measured in a field of 1.5 T in the temperature range of 10–200 K.

was previously observed in Ni–SiO_2 metal nanocomposites above the percolation transition [15, 16], but the mechanism of the anomalous Hall effect is still unexplained. Meanwhile, scaling $\rho_H^a \propto \rho^m$ with $m \approx 0.4$ is well explained by the concepts of the suppression of the intrinsic mechanism of the anomalous Hall effect in contaminated metals under the strong scattering of charge carriers [14].

CONCLUSIONS

Thus, the transport properties and the anomalous Hall effect of film nanocomposites $(Co_{40}Fe_{40}B_{20})_x(AlO_y)_{100-x}$ and $(Co_{84}Nb_{14}Ta_2)_x(AlO_y)_{100-x}$ based on nonstoichiometric AlO_y oxide, containing a ferromagnetic metal, are studied near the metal–insulator transition ($57 > x > 47$ at %). The nanocomposites were prepared by the ion-beam sputtering of composite targets. The peculiarity of the method is that it enables the preparation of a composite system with a gradually varying ratio of metallic and insulating phases in a wide range (25–60 at %) in one technological cycle.

It is found that at the metal concentration of $57 > x > 49$ at %, the conductivity of nanocomposites is well described by logarithmic equation $\sigma(T) = a + b\ln T$, where parameter b is almost independent of x. This dependence, according to [2], is due to the peculiarities of the Coulomb interaction in the metal–insulator composite in the transition region form the metallic conductivity to the dielectric regime. It is demonstrated by using [2] that parameter b is determined by the characteristic size of the percolation cluster cell D, which is difficult to determine by electron microscopy near the percolation transition. In nanocomposites of both types, the found values of D were ~8 nm, which is consistent with the estimate of the granule size (2–7 nm) in these systems by electron microscopy [3].

The temperature dependence of the anomalous Hall effect in the case of the logarithmic dependence of the conductivity is studied for the first time. It was found that near the metal–insulator transition, the parametric dependence of the anomalous Hall effect ρ_H^a on the longitudinal resistance $\rho(T)$ is a power law with the exponent $m \approx 0.4$, which is explained by the suppression of the intrinsic mechanism of the anomalous Hall effect under the strong scattering of charge carriers [14].

These results are of great importance for creating nanocomposite devices based on nonlinear effects, in particular, memristors, that are most strongly manifested near the percolation threshold.

ACKNOWLEDGMENTS

The work was supported by the Russian Science Foundation, project no. 16-19-10233.

REFERENCES

1. X. Batlle and A. Labarta, J. Phys. D: Appl. Phys. **35**, R15 (2002).
2. I. S. Beloborodov, A. V. Lopatin, V. M. Vinokur, and K. B. Efetov, Rev. Mod. Phys. **79**, 469 (2007).
3. S. A. Gridnev, Yu. E. Kalinin, and A. V. Sitnikov, *Nonlinear Phenomena in Nano- and Microheterogeneous Systems* (BINOM. Laboratoriya Znanii, Moscow, 2012). [in Russian].
4. A. Milner, A. Gerber, B. Groisman, M. Karpovsky, and A. Gladkikh, Phys. Rev. Lett. **76** (3), 475 (1996).
5. P. Krzysteczko, G. Reiss, and A. Thomas, Appl. Phys. Lett. **95**, 112508 (2009).
6. K. B. Efetov and A. Tschersich, Phys. Rev. B **67**, 174205 (2003).
7. Yu. E. Kalinin, A. N. Remizov, and A. V. Sitnikov, Phys. Solid State **46**, 2146 (2004).
8. Yu. O. Mikhailovskii, V. N. Prudnikov, V. V. Ryl'kov, K. Yu. Chernoglazov, A. V. Sitnikov, Yu. E. Kalinin, and A. B. Granovskii, Phys. Solid State **58** (3), 444 (2016).
9. N. Nagaosa, J. Sinova, S. Onoda, A. H. MacDonald, and N. P. Ong, Rev. Mod. Phys. **82**, 1539 (2010).
10. T. Fukumura, H. Toyosaki, K. Ueno, M. Nakano, T. Yamasaki, and M. Kawasaki, Jpn. J. Appl. Phys. **46**, L642 (2007).
11. A. Fernández-Pacheco, J. M. De Teresa, J. Orna, L. Morellon, P. A. Algarabel, J. A. Pardo, and M. R. Ibarra, Phys. Rev. B **77**, 100403(R) (2008).
12. M. Glunk, J. Daeubler, W. Schoch, R. Sauer, and W. Limmer, Phys. Rev. B **80**, 125204 (2009).
13. D. Chiba, A. Werpachowska, M. Endo, Y. Nishitani, F. Matsukura, T. Dietl, and H. Ohno, Phys. Rev. Lett. **104**, 106601 (2010).
14. S. Onoda, N. Sugimoto, and N. Nagaosa, Phys. Rev. B **77**, 165103 (2008).
15. A. Pakhomov, X. Yan, and B. Zhao, Appl. Phys. Lett. **67**, 3497 (1995).
16. D. Bartov, A. Segai, M. Karpovski, and A. Gerber, Phys. Rev. B **90**, 144423 (2014).

Translated by O. Zhukova